Effective Field Theory and Finite-Density Systems

Richard J. Furnstahl,[1] Gautam Rupak,[2] and Thomas Schäfer[2]

[1]Department of Physics, Ohio State University, Columbus, Ohio 43210; email: furnstahl.1@osu.edu

[2]Department of Physics, North Carolina State University, Raleigh, North Carolina 27695; email: grupak@gmail.com, tmschaef@ncsu.edu

Annu. Rev. Nucl. Part. Sci. 2008. 58:1–25

First published online as a Review in Advance on April 17, 2008

The *Annual Review of Nuclear and Particle Science* is online at nucl.annualreviews.org

This article's doi: 10.1146/annurev.nucl.58.110707.171142

0163-8998/08/1123-0001$20.00

Key Words

nuclear matter, many-body physics, chiral symmetry

Abstract

This review gives an overview of effective field theory (EFT) as applied at finite density, with a focus on nuclear many-body systems. Uniform systems with short-range interactions illustrate the ingredients and virtues of many-body EFT; we also survey the varied frontiers of EFT for finite nuclei and nuclear matter.

Contents

1. INTRODUCTION

Calculating the properties of atomic nuclei and nuclear matter starting from microscopic internucleon forces is one of the oldest unsolved challenges of nuclear physics. Renewed interest in this problem has been fueled by experiments at rare isotope facilities, which are opening the door to new domains of unstable nuclides that are not all accessible in the lab, and by descriptions of astrophysical phenomena such as supernovae and neutron stars, which require controlled extrapolations of the equation of state of nuclear matter in density, temperature, and proton fraction (1). Despite decades of work and technological advances, however, there remain severe computational barriers and only limited control of uncertainties in conventional nuclear many-body calculations of all but the lightest nuclei. The difficulties are exacerbated by the need to supplement accurate phenomenological two-nucleon potentials with poorly understood many-body forces to achieve a quantitative (and in many cases qualitative) description of nuclei. Finally, conventional approaches are at best loosely connected to quantum chromodynamics (QCD), the underlying theory of the strong interaction.

Effective field theory (EFT) provides new tools to address these challenges. The goal of EFT applied to finite-density nuclear systems is to place nuclear many-body physics on a firm foundation so that it can be (*a*) systematically improved with associated theoretical error bars, (*b*) extended reliably to regimes where there are limited or no data, and (*c*) connected to QCD as well as to few-body experiments. In this review, we aim to describe how EFT can accomplish these goals in many-body systems and to survey the frontiers of EFT-based calculations of many-body nuclei and nuclear matter.

Any EFT builds on a basic physics principle that underlies every low-energy effective model or theory. A high-energy, short-wavelength probe reveals details down to scales comparable to the wavelength. Thus, electron scattering at sufficiently high energy reveals the quark substructure of protons and neutrons in a nucleus. At lower energies, however, details are not resolved, and one can replace short-distance structure with something simpler, as in a multipole expansion of a complicated charge or current distribution. This means that it is not necessary to calculate with full QCD to do accurate strong interaction physics at low energies; one can replace quarks and gluons by neutrons and protons (and maybe pions, nucleon resonances, etc.). EFT provides a

systematic, model-independent way to carry out this program starting with a local Lagrangian framework.

An EFT is formulated by specifying appropriate low-energy degrees of freedom and then constructing the Lagrangian as a complete set of terms that embodies the symmetries of the underlying theory. (Note that the general Lagrangian will typically be overcomplete, but redundant terms can be removed by redefining the fields appropriately.) There is no unique EFT for nuclear physics. In different applications the relevant degrees of freedom might be neutrons and protons only; neutrons, protons, and pions; or neutrons, protons, pions, and Δs or quasi-nucleons. The form of the EFT can be chosen to readily expose universal behavior; for instance, dilute neutron matter has features in common with phenomena seen in cold atom experiments.

In applying an EFT Lagrangian, one must confront in a controlled way the impact of excluded short-distance physics. Quantum mechanics implies that sensitivity to short-distance physics is always present in a low-energy theory, but that it is made manifest in an EFT through dependence on a cutoff or other regulator instead of being hidden in phenomenological form factors. Removing this dependence necessitates a well-defined regularization and renormalization scheme as part of the EFT specification. This necessity becomes a virtue as residual regulator dependence can be used to assess truncation errors and many-body approximations. Furthermore, the freedom in regulating coupled with the freedom in making unitary transformations can be exploited by renormalization group (RG) methods to greatly simplify few- and many-body nuclear calculations.

For an EFT calculation to be improvable order by order, one needs a scheme to organize the infinite possible terms in the Lagrangian based on an expansion parameter (or parameters). Such a scheme is called a power counting. Power counting tells us what terms (or Feynman diagrams) to include at each order and lets us estimate the theoretical truncation error. The radius of convergence associated with the expansion means that the EFT predicts its own downfall, in contrast to phenomenological models. EFT expansion parameters most commonly arise as a ratio of disparate physical scales rather than as a small coupling constant (e.g., as in Coulomb systems); a many-body example is the ratio of the range of the interaction to the interparticle spacing in a dilute system. The power counting for this example is particularly simple when the scattering length is roughly the same size as the interaction range (called natural) but changes dramatically if the scattering length is much larger (called unnatural). We explore both scenarios below.

Chiral EFT is a faithful low-energy realization of QCD whose power counting takes advantage of the spontaneously broken chiral symmetry that gives rise to the almost massless (on hadronic scales) pion. It has the potential to bridge the gap between QCD and nuclei, letting us explore how nuclear properties depend on QCD parameters (e.g., how the binding energies of nuclei would change if the light quark masses were different or if the QCD scale parameter were time dependent) and opening a connection to ab initio QCD lattice calculations. Chiral EFT power counting explains the empirical hierarchy of many-body forces in nuclear physics, fixes their natural sizes, and gives an organizing principle for their construction. Other compelling features are the systematic inclusion of relativistic corrections and prescriptions for consistent currents needed to predict experimental observables.

A comprehensive treatment of EFT and finite-density nuclear systems would require several extended reviews covering EFT in general, EFT applied to internucleon interactions, and field theory at finite density. Fortunately, recent articles in this journal provide much of the background for the interested reader; these include an introduction to EFT by Burgess (2), an overview of chiral perturbation theory by Bernard & Meißner (3), and a review of EFT for few-nucleon systems by Bedaque & van Kolck (4) (see also References 5 and 6). We focus here on illustrating how the basic principles of EFT can be realized at finite density and on surveying various applications to

nuclear matter and finite nuclei. Our treatment is schematic in most cases and we refer the reader to the literature for details.

In Section 2, we consider uniform systems with short-range interactions. The dilute Fermi gas with repulsive interactions serves as a prototype for EFT at finite density, whereas new features and techniques arise when we study physics near the Fermi surface. Many-body systems with unnatural scattering lengths, which manifest various forms of universal physics, are attacked by a variety of nonperturbative EFT techniques. Actual applications of EFT to nuclear many-body systems are in their infancy and there are multiple frontiers; we describe a range of examples in Section 3. These include the use of chiral EFT interactions as input to conventional many-body wave function methods applicable to light nuclei and a pioneering attempt to apply EFT to the methods themselves. Lattice calculations provide a complementary nonperturbative approach. Perturbative chiral EFT calculations for nuclei may be possible, however, if the power counting differs at nuclear densities. This may be justified by RG transformations that soften the chiral interactions. Finally we discuss density functional theory (DFT), which is computationally tractable for all nuclides and is naturally cast in EFT form using effective actions. In Section 4 we conclude with a summary of the current status of EFT for nuclear systems, ongoing developments, important open questions, and a brief discussion of omitted topics.

2. EFFECTIVE FIELD THEORY FOR UNIFORM SYSTEMS

In this section, we illustrate the ideas of EFT at finite density for uniform systems with short-range interactions.

2.1. Prototype Many-Body Effective Field Theory

We start with the simplest possible application, a dilute Fermi system with repulsive, spin-independent interactions of range R. A concrete example is "hard-sphere" repulsion at radius R, which can be viewed as a caricature of the short-range part of the nuclear force. In perturbation theory all matrix elements of this potential are infinite; whereas a more realistic potential would not be so extreme, textbook treatments of this many-body problem all start with nonperturbative summations and then expansions at low density (7). In contrast, the EFT approach directly exploits the essential physics result that low-momentum nucleons do not resolve the hard core.

With either approach, the end result for free-space, two-particle scattering at low energies ($\lambda = 2\pi/k \gg 1/R$) is the effective range expansion; e.g., the s-wave phase shift $\delta_0(k)$ satisfies:

$$k \cot \delta_0(k) \stackrel{k\to 0}{\to} -\frac{1}{a_0} + \frac{1}{2} r_0 k^2 + \ldots, \qquad 1.$$

where a_0 is the scattering length and r_0 is the effective range. The system is said to have a natural scattering length if it is the same order as the range of the interaction (e.g., $a_0 = R$ and $r_0 = 2R/3$ for hard spheres). Below we consider the case of unnatural scattering length, with $a_0 \gg R$, which is relevant for dilute neutron matter and cold atom systems. For a natural system, the dilute expansion of the energy density for a uniform system starts as (s-wave only here)

$$\mathcal{E} = \rho \frac{k_F^2}{2M} \left[\frac{3}{5} + (\nu - 1) \left\{ \frac{2}{3\pi}(k_F a_0) + \frac{4}{35\pi^2}(11 - 2\ln 2)(k_F a_0)^2 + \frac{1}{10\pi}(k_F r_0)(k_F a_0)^2 \right\} + \cdots \right], \qquad 2.$$

where k_F is the Fermi momentum, ν is the spin degeneracy, and $\rho = \nu k_F^3/6\pi^2$. This result arises very cleanly from an EFT treatment (8).

Consider the ingredients for any EFT along with the specifics for this example:

1. Use the most general $\mathcal{L}$ with low-energy degrees of freedom consistent with global and local symmetries of the underlying theory. Here we have nucleons only with Galilean invariance and discrete symmetries. A general interaction is then a sum of δ functions and derivatives of δ functions with two-body interactions (four fields), three-body interactions (six fields), and so on. Therefore, $\mathcal{L}_{\rm eft}$ is

$$\mathcal{L}_{\rm eft} = \psi^\dagger \left[i\frac{\partial}{\partial t} + \frac{\nabla^2}{2M} \right] \psi - \frac{C_0}{2}(\psi^\dagger\psi)^2 + \frac{C_2}{16}[(\psi\psi)^\dagger(\psi \overleftrightarrow{\nabla}^2 \psi) + \text{h.c.}] - \frac{D_0}{6}(\psi^\dagger\psi)^3 + \ldots, \quad 3.$$

   where ... indicates terms with more derivatives and more fields. (We have eliminated higher-order time derivatives using the equations of motion; see Reference 8.) The ψs have ν components and spin-indices are implicit (and contracted between $\psi^\dagger$ and ψ).
2. Declare a regularization and renormalization scheme. One choice is to smear out the δ functions (e.g., as Gaussians in momentum space) to introduce a cutoff; renormalization would remove cutoff dependence. However, for a natural a_0, using dimensional regularization and minimal subtraction (rather than a cutoff) is particularly convenient and efficient.
3. Establish a well-defined power counting, which means identifying small expansion parameters, typically using a ratio of scales. In free space k/Λ with $\Lambda \sim 1/R$ is the clear choice, and then k_F/Λ is the corresponding parameter in the medium. Dimensional analysis, with some additional insight to give us the 4πs, implies ($2i$ denotes the number of gradients)

$$C_{2i} \sim \frac{4\pi}{M} R^{2i+1}, \quad D_{2i} \sim \frac{4\pi}{M} R^{2i+4}, \quad 4.$$

   which will enable us to make quantitative power-counting estimates.

Feynman diagrams and rules for the EFT follow from conventional formalism for free-space and many-body perturbation theory (see, e.g., References 7 and 9). The constants C_{2i} are determined by matching to the free-space scattering amplitude $f_0(k)$ in perturbation theory:

$$f_0(k) = \frac{4\pi}{M}\left(a_0 - ia_0^2 k - a_0^3 k^2 + a_0^2 r_0 k^2 + \cdots\right). \quad 5.$$

The leading potential $V^{(0)}_{\rm EFT}(\mathbf{x}) = C_0\delta(\mathbf{x})$ or $\langle \mathbf{k}|V^{(0)}_{\rm eft}|\mathbf{k}'\rangle = C_0$, where $\mathbf{k}, \mathbf{k}'$ are relative momenta. Matching to $f_0(k)$ fixes $C_0 = 4\pi a_0/M$ at leading order (LO), which then determines the leading finite-density contribution (Hartree-Fock) in Equation 2 after sums over the Fermi sea:

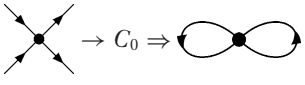

$$\to C_0 \Rightarrow \to \mathcal{E}_{\rm LO} = \frac{C_0}{2}\nu(\nu-1)\left(\sum_{\mathbf{k}}^{k_F} 1\right)^2 \propto a_0 k_F^6. \quad 6.$$

Similar matching yields C_2 in terms of a_0 and r_0 and the corresponding Hartree-Fock contribution for the effective range.

At the next order is $\langle \mathbf{k}|V^{(0)}_{\rm eft} G_0 V^{(0)}_{\rm eft}|\mathbf{k}'\rangle$, which includes a linearly divergent loop integral:

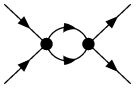

$$\to C_0 M \int^{\Lambda_c} \frac{d^3q}{(2\pi)^3}\frac{1}{k^2 - q^2 + i\varepsilon} C_0 = C_0^2 M\left(\frac{\Lambda_c}{2\pi^2} - \frac{ik}{4\pi} + \mathcal{O}\left(\frac{k^2}{\Lambda_c}\right)\right). \quad 7.$$

We can redefine (renormalize) C_0 to absorb the linear dependence on the cutoff Λ_c, but we will obtain higher powers of k from every diagram. A more efficient scheme is dimensional regularization

with minimal subtraction (DR/MS), which implies that only one power of k survives:

$$\int \frac{d^D q}{(2\pi)^3} \frac{1}{k^2 - q^2 + i\varepsilon} \overset{D\to 3}{\to} -\frac{ik}{4\pi}. \qquad 8.$$

Thus we obtain the second term in Equation 5 automatically with no change in C_0. At higher orders there is exactly one power of k per diagram and natural coefficients (i.e., consistent with Equation 4), so we can estimate truncation errors from simple dimensional analysis.

The contribution to the energy density has two terms, one of which vanishes identically. In the other, we again obtain a linear divergence,

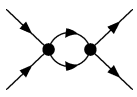

$$\Rightarrow \mathcal{E}_{\rm NLO} \propto \int_{k_{\rm F}}^{\infty} \frac{d^3 q}{(2\pi)^3} \frac{C_0^2}{k^2 - q^2}, \qquad 9.$$

but the same renormalization fixes it,

$$\int_{k_{\rm F}}^{\infty} \frac{1}{k^2 - q^2} = \int_0^{\infty} \frac{1}{k^2 - q^2} - \int_0^{k_{\rm F}} \frac{1}{k^2 - q^2} \overset{D\to 3}{\to} - \int_0^{k_{\rm F}} \frac{1}{k^2 - q^2}, \qquad 10.$$

and particles become holes through the renormalization. Pauli blocking does not change the free-space UV (short-distance) renormalization as the density is a long-distance effect; after fixing free space, the in-medium renormalization is determined. We find $\mathcal{E}_{\rm NLO} \propto a_0^2 k_{\rm F}^7$.

The diagrammatic power counting with DR/MS is very simple, with each loop adding a power of k in free space. At finite density, a diagram with V_{2i}^n n–body vertices and $2i$ gradients scales as $(k_{\rm F})^\beta$ with

$$\beta = 5 + \sum_{n=2}^{\infty} \sum_{i=0}^{\infty} (3n + 2i - 5) V_{2i}^n. \qquad 11.$$

This reproduces, for example, the LO [$\beta = 5 + (3 \cdot 2 + 2 \cdot 0 - 5) \cdot 1 = 6$] and next-to-leading order (NLO) [$\beta = 5 + (3 \cdot 2 + 2 \cdot 0 - 5) \cdot 2 = 7$] dependencies. The power counting is exceptionally clean, with a separation of vertex factors $\propto a_0, r_0, \ldots$ and a dimensionless geometric integral multiplying $k_{\rm F}^\beta$, with each diagram contributing to exactly one order in the expansion. There is a systematic hierarchy, as adding derivatives or higher-body interactions increases the power of $k_{\rm F}$. The ratio of successive terms is $\sim k_{\rm F} R$ (see, e.g., Equation 2), so we can estimate excluded contributions.

The energy density (2) looks like a power series in $k_{\rm F}$, but at higher order there are logarithmic divergences from 3–3 scattering, which indicate new sensitivity to short-distance behavior. A cutoff Λ_c serves as a resolution scale; as we increase Λ_c, we see more of the short-distance details. Observables (such as scattering amplitudes) must not vary with Λ_c, so changes must be absorbed in a coupling. But the coupling cannot be from 2–2 scattering, as we already regularized all the divergences there. Instead, we must use the point-like three-body force, whose coupling $D_0(\Lambda_c)$ can absorb the dependence on Λ_c (10). The diagrams are $\propto (C_0)^4 \ln(k/\Lambda_c)$, which means that

$$\frac{d}{d\Lambda_c}$$

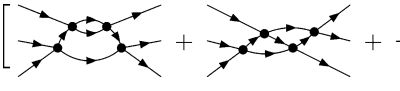

$$= 0 \Rightarrow D_0(\Lambda_c) \propto (C_0)^4 \ln(a_0 \Lambda_c) \qquad 12.$$

fixes the coefficient $D_0(\Lambda_c)$. Dimensional regularization works similarly (8). In turn this implies the following result for the energy density:

$$\mathcal{O}\left(k_{\rm F}^9 \ln(k_{\rm F})\right):$$

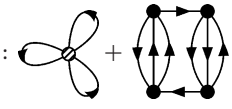

$$+ \cdots \propto (\nu - 2)(\nu - 1) k_{\rm F}^5 (k_{\rm F} a_0)^4 \ln(k_{\rm F} a_0) \qquad 13.$$

without actually carrying out the calculation! Similar analyses can identify the higher logarithmic terms in the expansion of the energy density (8, 10). This example illustrates the inevitability of many-body forces in low-energy theories: When the resolution or degrees of freedom are changed, we will have many-body forces. Thus the question is not whether such forces are present, but how large they are. For nuclear physics, their natural size implies that they cannot be neglected.

This brief tour of the EFT for a natural dilute Fermi gas includes features common to many other applications. Even if we know that the underlying physics is a hard-sphere potential, the EFT is easier to calculate than conventional approaches (7). Further, the EFT directly reveals the universal nature of the many-body counterpart to the effective range expansion, which applies to any short-range repulsive potential. Of course, this example is very simple; there are many ways to generalize. Some are immediate: For instance, we can account for short-range spin-dependent interactions by adding terms such as $C_0^{\sigma}(\psi^\dagger \boldsymbol{\sigma}\psi)\cdot(\psi^\dagger\boldsymbol{\sigma}\psi)$. To consider unnatural scattering, however, we must revisit the power counting and consider alternative expansion parameters, as $k_{\rm F}a_0$ is no longer small. But first we turn from EFT for bulk properties to EFT near the Fermi surface.

2.2. Effective Field Theory Near the Fermi Surface

The theory described in the last section is completely perturbative. At any order in the $k_{\rm F}R$ expansion, only a finite number of diagrams need to be computed. There are two ways in which this expansion can fail. One possibility is that one of the effective range parameters (typically, the scattering length) is anomalously large, so that a certain class of diagrams must be summed to all orders. We examine this problem in Section 2.3. A second possibility is that the density (and the Fermi momentum) is too large and that $k_{\rm F}R$ ceases to be a useful expansion parameter. In this case it is possible to construct a different kind of EFT by focusing on quasi-particles in the vicinity of the Fermi surface and using $|k-k_{\rm F}|/\Lambda$ as an expansion parameter. This effective theory is known as Landau Fermi-liquid theory (11, 12). The Landau theory does not account for all properties of the many-body system, but it does describe phenomena that are sensitive to physics near the Fermi surface such as collective modes, pairing, and transport properties.

Fermi-liquid theory was originally developed by Landau using intuitive arguments. These arguments were later confirmed by Abrikosov and others using diagrammatic many-body perturbation theory (13). The modern view of Fermi-liquid theory as an EFT was advocated by Shankar, Polchinski, and others (14, 15). Consider the effective action of noninteracting, nonrelativistic fermions near a Fermi surface,

$$S=\int dt\int\frac{d^3p}{(2\pi)^3}\psi^\dagger(p)\left(i\frac{\partial}{\partial t}-v_{\rm F}l_p\right)\psi(p). \qquad 14.$$

Here we have decomposed the momenta as $\mathbf{p}=\mathbf{k}+\mathbf{l}_p$, where $\mathbf{k}$ is on the Fermi surface, $|\mathbf{k}|=k_{\rm F}$, and $\mathbf{l}_p$ is orthogonal to the Fermi surface. The Fermi velocity is defined as $v_{\rm F}=\partial E_p/\partial p$, where E_p is the quasi-particle energy. The power counting can be established by studying the behavior of the operators under transformations $l_p\to sl_p$ that scale the momenta towards the Fermi surface. In writing $E_p=E_{\rm F}+v_{\rm F}l_p+\mathcal{O}(l_p^2)$, we see that as $s\to 0$ only the Fermi velocity survives, so the detailed form of the dispersion relation is irrelevant. Using $d^3p=k_{\rm F}^2(dl_p)(d\Omega)$, we observe that $d^3p\sim s$, $dt\sim s^{-1}$, $\psi\sim s^{-1/2}$, and that S in (14) is $\mathcal{O}(s^0)$.

We now turn to the importance of interactions between fermions near the Fermi surface. The most general four-fermion interaction is of the form

$$S_{4f}=\frac{1}{4}\int dt\left[\prod_{i=1}^{4}\int\frac{d^3p_i}{(2\pi)^3}\right]\psi^\dagger(\mathbf{p}_4)\psi^\dagger(\mathbf{p}_3)\psi(\mathbf{p}_2)\psi(\mathbf{p}_1)\delta^3\left(\mathbf{p}_{\rm tot}\right)U(\mathbf{p}_4,\mathbf{p}_3,\mathbf{p}_2,\mathbf{p}_1), \qquad 15.$$

where $\mathbf{p}_{\rm tot}$ is the sum of the four momenta $\mathbf{p}_i$, and we have suppressed the spin labels on U. For a generic set of momenta $\mathbf{p}_i$ the δ function constrains the large components of the momenta and scales as $\delta^3(\mathbf{p}_{\rm tot}) \sim s^0$. In this case the four-fermion interaction scales as s^1 and becomes irrelevant near the Fermi surface. Interactions involving more fermions are even more strongly suppressed.

An exception occurs if the large components of the momenta cancel. This happens for back-to-back momenta, $\mathbf{k}_1 = -\mathbf{k}_2$, and for generalized forward scattering, $\mathbf{k}_1 \cdot \mathbf{k}_2 = \mathbf{k}_3 \cdot \mathbf{k}_4$. In these cases one component of the δ functions constrains $\mathbf{l}$, the scaling of the δ function is changed to s^{-1}, and the four-fermion interaction is marginal, $S_{4f} \sim s^0$. Whether or not the four-fermion interaction qualitatively changes the theory of noninteracting quasi-particles described by Equation 14 depends on quantum corrections, which can change the scaling from marginal to marginally relevant [$S_{4f} \sim \log(s)$] or irrelevant [$S_{4f} \sim \log(s)^{-1}$].

The one-loop corrections to the four-fermion interaction are given by

$\delta S_{BCS} \sim$ 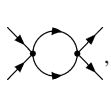 , $\delta S_{ZS} \sim$ 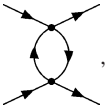 , $\delta S_{ZS'} \sim$ 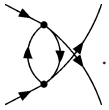 . 16.

There are two possible scenarios. One possibility is that the interaction in the Bardeen-Cooper-Schrieffer (BCS) channel ($\mathbf{k}_1 = -\mathbf{k}_2$) is attractive in some partial wave. In this case the first diagram in Equation 16 leads to a logarithmic growth of the interaction. We can illustrate this effect using the s-wave four-fermion interaction defined in Equation 3. For $\mathbf{p}_1 = -\mathbf{p}_2$ and $E_1 = E_2 = E$, the one-loop correction to C_0 is given by

$$-C_0^2 \left(\frac{k_{\rm F} m}{2\pi^2}\right) \log\left(\frac{E_0}{E}\right), \qquad 17.$$

where E_0 is a UV cutoff. This result can be interpreted as an effective energy-dependent coupling. The coupling constant satisfies the RG equation

$$E\frac{dC_0}{dE} = C_0^2 \left(\frac{k_{\rm F} m}{2\pi^2}\right) \Rightarrow C_0(E) = \frac{C_0(E_0)}{1 + NC_0(E_0)\log(E_0/E)}, \qquad 18.$$

where $N = k_{\rm F} m/2\pi^2$ is the density of states. Equation 18 shows that if the initial coupling is repulsive, $C_0(E_0) > 0$, then the RG evolution will drive the effective coupling to zero. If, on the other hand, the initial coupling is attractive, $C_0(E_0) < 0$, then the effective coupling will grow and reach a pole (called a Landau pole) at $E_{crit} \sim E_0 \exp(-1/(N|C_0(E_0))))$. At the Landau pole the effective theory defined by Equations 14 and 15 has to break down. The RG equation does not determine what happens at this point, but we can assume that the strong attractive interaction leads to the formation of a fermion pair condensate in the BCS channel $\langle\psi(\mathbf{p})\psi(-\mathbf{p})\rangle$. The magnitude of the difermion condensate as well as the corresponding gap in the energy spectrum is easiest to compute if the microscopic interaction is weak (i.e., if $k_f R < 1$). Employing standard methods, we derive the gap equation

$$1 = \frac{|C_0|}{2} \int \frac{d^3p}{(2\pi)^3} \frac{1}{\sqrt{(E_p - E_F)^2 + \Delta^2}}. \qquad 19.$$

The infrared divergence in the BCS channel is regulated by the energy gap Δ. The gap equation also has a logarithmic UV divergence. This divergence can be treated consistently with the relation between C_0 and a_0 derived in Section 2.1 by using dimensional regularization (16, 17). The result is

$$\Delta = \frac{8E_{\rm F}}{e^2} \exp\left(-\frac{\pi}{2k_{\rm F}|a_0|}\right). \qquad 20.$$

The term in the exponent represents the leading term in an expansion in $k_F|a_0|$. This means that in order to determine the pre-exponent in Equation 20 we must solve the gap equation at NLO. This correction corresponds to keeping the zero sound diagram in Equation 16. In nuclear physics this term is known as the induced interaction (18). For zero-range potentials, the induced interaction was first computed by Gorkov & Melik-Barkhudarov (19). It leads to a suppression of the *s*-wave gap by a factor $(4e)^{1/3} \simeq 2.2$.

For nuclear matter the result given in Equation 20 is not very useful, both because the scattering length is large and because effective range corrections are not negligible. We discuss the pairing gap in the limit $a_0 \to \infty$ in Section 2.3. Range corrections in the case of a normal scattering length were studied in Reference 16. A rough estimate of the gap at moderate densities can be obtained by replacing $1/(k_F a)$ with $\cot[\delta_0(k_F)]$, where $\delta_0(k)$ is the *s*-wave phase shift. This estimate gives neutron gaps on the order of 1 MeV at nuclear-matter density.

The second scenario arises if the interaction in the BCS channel is either repulsive or very weak. In this case the forward-scattering amplitudes are important. The interaction is

$$U(\hat{p}_4,\ \hat{p}_3,\ \hat{p}_2,\ \hat{p}_1)|_{\hat{p}_1\cdot\hat{p}_2=\hat{p}_3\cdot\hat{p}_4} = F(\hat{p}_1\cdot\hat{p}_2, \phi_{12,34}), \qquad 21.$$

where $\phi_{12,34}$ is the angle of the plane spanned by $\mathbf{p}_{1,2}$ and $\mathbf{p}_{3,4}$. The function $F(x, 0)$ is called the Landau function and its Legendre coefficients are referred to as Landau parameters. If spin dependence is included, there is a second set of Landau parameters commonly denoted F_l'. The Landau parameters remain marginal at one-loop order.

The EFT characterized by v_F and F_l is called the Landau Fermi-liquid theory (11, 12). The Landau parameters can be related to compressibility, the velocity of zero and first sound, transport coefficients, etc. The compressibility of nuclear matter, for example, is given by

$$\frac{dP}{d\rho} = \frac{k_F^2}{m^2}\frac{1+F_0}{3+F_1}. \qquad 22.$$

The coefficient F_i can be extracted from experiment, but ultimately we would like to find a systematic method for computing the Landau parameters from the underlying nucleon-nucleon interaction. One possibility is to use the RG to integrate out modes far away from the Fermi surface. A difficulty with this strategy is the problem of finding suitable initial conditions for the RG flow. Schwenk et al. (20) proposed to use a free-space RG to generate a universal low-momentum effective interaction $V_{\mathrm{low}\,k}$ (which we discuss in more detail in Section 3.2). This interaction, evolved to a scale $\Lambda \sim 2k_F$, can be used as a starting point for the determination of the Landau parameters (20).

2.3. Unnatural Scattering Length

An important aspect of nuclear physics is the fact that the nucleon scattering lengths are anomalously large. The neutron-proton scattering length in the $^1S_0$ channel is -23.71 fm, and the binding energy in the $^3S_1$ (deuteron) channel is 2.2 MeV. This implies that expanding the scattering amplitudes in powers of the momentum (as in Equation 5) is not useful, and that powers of $a_0 k$ have to be kept to all orders. Keeping the first two terms in the effective range expansion, the scattering amplitude can be written as

$$f_0(k) \sim \frac{1}{-1/a_0 + r_0 k^2/2 - ik} = \frac{1}{-1/a_0 - ik}\left\{1 + \frac{r_0/2}{-1/a_0 - ik} + \ldots\right\}. \qquad 23.$$

This expansion can be reproduced by keeping the *s*-wave contact interaction proportional to C_0 to all orders, and treating C_{2i} $(i > 0)$ perturbatively as before. This procedure gives the correct result,

but in dimensional regularization (with minimal subtraction) or cutoff regularization the power counting of individual diagrams is not manifest. This is readily seen in dimensional regularization where $C_0 \to \infty$ as $a_0 \to \infty$. As a consequence, individual diagrams diverge in the limit of a large scattering length even though the sum of all diagrams is finite. Kaplan et al. proposed a modified version of dimensional regularization (power divergence subtraction, or PDS) in which poles in lower dimensions are subtracted and power counting is manifest (21).

Interest in many-body systems with a large two-particle scattering length arises not only in nuclear physics, but also in atomic physics. It is now possible to create cold atomic gases in which the scattering length a_0 of the atoms can be adjusted experimentally using Feshbach resonances (see Reference 22 for a review). If the density is low, the atoms can be described as pointlike nonrelativistic particles that carry a "spin" label that characterizes the hyperfine quantum numbers of the atoms. A Feshbach resonance arises if a molecular bound state in a closed hyperfine channel crosses near the threshold of a lower "open" channel. Because the magnetic moments of the open and closed states are usually different, Feshbach resonances can be tuned using an applied magnetic field. At resonance the two-body scattering length in the open channel diverges, and the cross section σ is limited only by unitarity; $\sigma(k) = 4\pi/k^2$ for low momenta k. In the unitarity limit, details about the microscopic interaction are lost, and the system displays universal properties.

A dilute gas of any fermions in the unitarity limit is a strongly coupled quantum liquid that exhibits universality. At low density the limit $k_F a_0 \to \infty$ and $k_F r_0 \to 0$ is particularly interesting. From dimensional analysis it is clear that the energy per particle at zero temperature must be proportional to the energy per particle of a free Fermi gas at the same density:

$$\frac{E}{A} = \xi \left(\frac{E}{A}\right)_0 = \xi \frac{3}{5}\left(\frac{k_F^2}{2m}\right). \qquad 24.$$

The constant ξ is universal, that is, independent of the details of the system. Similar universal constants govern the magnitude of the gap in units of Fermi energy and the equation of state at finite temperature.

Calculating these universal constants is clearly a very challenging task—many-body diagrams containing C_0 must be summed to all orders. One possible solution is to do the calculation numerically, using diffusion or imaginary time path–integral Monte Carlo methods as described in Section 3.3. It would be desirable to find systematically improvable analytical approaches. Analytical methods offer the ability to systematically include higher-order terms in the interaction (range corrections, explicit pions, three-body forces, etc.) and to determine real-time properties that are hard to access numerically. A few analytical methods have been considered, such as an expansion in the number of fermion species (23, 24) or the number of spatial dimensions (which is related to the hole-line expansion of Brueckner, Bethe, and Goldstone; see References 25 and 26). Below, we discuss a proposal to perform an expansion around $d = 4 - \varepsilon$ spatial dimensions. ε expansions are well known in the theory of critical phenomena. An interesting aspect of the ε expansion in nuclear physics is that both many-body and few-body systems can be studied (27).

Nussinov & Nussinov observed that the fermion many-body system in the unitarity limit reduces to a free Fermi gas near $d = 2$ spatial dimensions and to a free Bose gas near $d = 4$ (28). Their argument was based on the behavior of the two-body wave function as the binding energy goes to zero. For $d = 2$ it is well known that the limit of zero binding energy corresponds to an arbitrarily weak potential. In $d = 4$ the two-body wave function at $a_0 = \infty$ displays a $1/r^2$ behavior and the normalization is concentrated near the origin. These observations suggest that the many-body system is equivalent to a gas of noninteracting bosons. A systematic expansion based on the observation of Nussinov & Nussinov was studied by Nishida & Son (29). In this section we explain their approach.

We begin by restating the argument of Nussinov & Nussinov in the language of EFT. For the sake of simplicity we work with dimensional regularization and minimal subtraction. In this case $a_0 \to \infty$ corresponds to $C_0 \to \infty$. The fermion-fermion scattering amplitude is given by

$$f(p_0, \mathbf{p}) = \left(\frac{4\pi}{m}\right)^{d/2} \left[\Gamma\left(1 - \frac{d}{2}\right)\right]^{-1} \frac{i}{(-p_0 + E_p/2 - i\delta)^{\frac{d}{2}-1}}, \qquad 25.$$

where $\delta \to 0+$. As a function of d the gamma function has poles at $d = 2, 4, \ldots$ and the scattering amplitude vanishes at these points. Near $d = 2$ the scattering amplitude is independent of energy and momentum. For $d = 4 - \varepsilon$ we find

$$f(p_0, \mathbf{p}) = \frac{8\pi^2\varepsilon}{m^2} \frac{i}{p_0 - E_p/2 + i\delta} + \mathcal{O}(\varepsilon^2). \qquad 26.$$

We observe that at LO in ε the scattering amplitude resembles the propagator of a boson with mass $2m$. The boson-fermion coupling is $g^2 = (8\pi^2\varepsilon)/m^2$ and vanishes as $\varepsilon \to 0$. This suggests that we can set up a perturbative expansion involving fermions of mass m weakly coupled to bosons of mass $2m$. A difermion field can be introduced using the Hubbard-Stratonovich trick. The difermion self-coupling is proportional to $1/C_0$ and vanishes in the unitarity limit. The Lagrangian is

$$\mathcal{L} = \Psi^\dagger \left[i\partial_0 + \sigma_3 \frac{\nabla^2}{2m} \right] \Psi + \mu \Psi^\dagger \sigma_3 \Psi + (\Psi^\dagger \sigma_+ \Psi \phi + h.c.), \qquad 27.$$

where $\Psi = (\psi_\uparrow, \psi_\downarrow^\dagger)^T$ is a two-component Nambu-Gorkov field, σ_i are Pauli matrices acting in the Nambu-Gorkov space, and $\sigma_\pm = (\sigma_1 \pm i\sigma_2)/2$.

In the superfluid phase ϕ acquires an expectation value. We write

$$\phi = \phi_0 + g\varphi, \quad g = \frac{\sqrt{8\pi^2\varepsilon}}{m} \left(\frac{m\phi_0}{2\pi}\right)^{\varepsilon/4}, \qquad 28.$$

where $\phi_0 = \langle\phi\rangle$. The scale $M^2 = m\phi_0/(2\pi)$ was introduced in order to have a correctly normalized boson field. The scale parameter is arbitrary, but this particular choice simplifies some of the algebra. In order to obtain a well-defined perturbative expansion we add and subtract a kinetic term for the boson field to the Lagrangian. We include the kinetic term in the free part of the Lagrangian

$$\mathcal{L}_0 = \Psi^\dagger \left[i\partial_0 + \sigma_3 \frac{\nabla^2}{2m} + \phi_0(\sigma_+ + \sigma_-) \right] \Psi + \varphi^\dagger \left(i\partial_0 + \frac{\nabla^2}{4m} \right) \varphi, \qquad 29.$$

and the interacting part is

$$\mathcal{L}_I = g\left(\Psi^\dagger \sigma_+ \Psi \varphi + \text{h.c.}\right) + \mu \Psi^\dagger \sigma_3 \Psi - \varphi^\dagger \left(i\partial_0 + \frac{\nabla^2}{4m} \right) \varphi. \qquad 30.$$

Note that the interacting part generates self-energy corrections to the boson propagator, which, by virtue of Equation 26, cancels against the kinetic term of boson field. We also include the chemical potential term in $\mathcal{L}_I$. This is motivated by the fact that near $d = 4$ the system reduces to a noninteracting Bose gas and $\mu \to 0$. We count μ as a quantity of $\mathcal{O}(\varepsilon)$.

The Feynman rules are quite simple. The fermion and boson propagators are

$$G(p_0, \mathbf{p}) = \frac{i}{p_0^2 - E_p^2 - \phi_0^2} \begin{bmatrix} p_0 + E_p & -\phi_0 \\ -\phi_0 & p_0 - E_p \end{bmatrix}, \qquad D(p_0, \mathbf{p}) = \frac{i}{p_0 - E_p/2}, \qquad 31.$$

and the fermion-boson vertices are $ig\sigma_\pm$. Insertions of the chemical potential are $i\mu\sigma_3$. Both g^2 and μ are corrections of order ε. There are a finite number of one-loop diagrams that generate $1/\varepsilon$ terms. All other diagrams are finite, and the ε expansion is well defined.

The ground-state energy is determined by diagrams with no external legs. The first diagram is the free fermion loop, which is $\mathcal{O}(1)$ in the ε expansion. We obtain

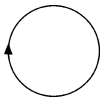

$$= -\int \frac{d^d p}{(2\pi)^d} \sqrt{E_p^2 + \phi_0^2} = \frac{\phi_0}{3}\left[1 + \frac{7 - 3(\gamma + \log(2))}{6}\varepsilon\right]\left(\frac{m\phi_0}{2\pi}\right)^{d/2}. \qquad 32.$$

An insertion of μ is also $\mathcal{O}(1)$ because the loop diagram is divergent in $d = 4$. We find

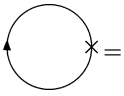

$$= \mu \int \frac{d^d p}{(2\pi)^d} \frac{E_p}{\sqrt{E_p^2 + \phi_0^2}} = -\frac{\mu}{\varepsilon}\left[1 + \frac{1 - 2(\gamma + \log(2))}{4}\varepsilon\right]\left(\frac{m\phi_0}{2\pi}\right)^{d/2}. \qquad 33.$$

Graphs with extra insertions of μ follow the naive ε counting and are at least $\mathcal{O}(\varepsilon^2)$. Nishida & Son (29) also computed the leading two-loop contribution, which is $\mathcal{O}(\varepsilon)$ because of the factor of g^2 from the vertices. The result is

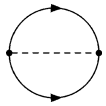

$$= -C_\varepsilon \left(\frac{m\phi_0}{2\pi}\right)^{d/2}, \qquad 34.$$

where the dashed line denotes the difermion propagator and $C \simeq 0.14424$.

We can now determine the minimum of the effective potential. We find $\phi_0 = (2\mu)/\varepsilon(1 + C'\varepsilon + \mathcal{O}(\varepsilon^2))$ with $C' = 3C - 1 + \log(2)$. The value of the effective potential at ϕ_0 determines the pressure and $n = \partial P/\partial\mu$ gives the density. From the density we can compute the Fermi momentum ($n \sim k_F^d$ in d dimensions), and the relationship between the Fermi energy $\varepsilon_F = k_F^2/2m$ and μ determines the universal parameter $\xi = \mu/\varepsilon_F$. We find

$$\xi = \frac{1}{2}\varepsilon^{3/2} + \frac{1}{16}\varepsilon^{5/2}\log(\varepsilon) - 0.025\varepsilon^{5/2} + \cdots = 0.475 \quad (\varepsilon = 1), \qquad 35.$$

which agrees quite well with the result of fixed-node quantum Monte Carlo calculations. The calculation was extended to $\mathcal{O}(\varepsilon^{7/2})$ by Arnold et al. (30). Unfortunately, the next term is very large and it appears necessary to combine the expansion in $4 - \varepsilon$ dimensions with a $2 + \varepsilon$ expansion in order to extract useful results. The ε expansion has also been applied to the calculation of the gap (29). At NLO the result is $\Delta = 0.62\varepsilon_F$. Somewhat surprisingly, this result is quite close to the naive $a_0 \to \infty$ limit of the BCS result given in Equation 20, provided that the induced interaction term is taken into account.

3. EFFECTIVE FIELD THEORY FOR FINITE NUCLEI AND NUCLEAR MATTER

In this section, we survey the wide range of pioneering applications of EFT to nonrelativistic finite-density nuclear systems. These frontiers are rapidly evolving and most results are immature, so we focus on general illustrative aspects.

3.1. Pion Physics from Chiral Effective Field Theory

To apply EFT to finite nuclei and nuclear matter, we must first consider the appropriate degrees of freedom. Applications to sufficiently low density systems such as dilute neutron matter are possible with nucleons as the only degrees of freedom. These are called pionless EFTs. In such an EFT, the pion is a heavy degree of freedom whose effects are mimicked by contact terms. This EFT breaks down when external momenta are comparable to the pion mass, and pion exchange

is resolved. This criterion does not automatically translate into a clear limit on the applicability of pionless EFT to finite nuclei; pionless EFT is successful for at least the ground states of the deuteron and triton, and its limits for heavier nuclei are not yet known (4).

However, given that the Fermi momentum k_F for the interior of heavy nuclei is about twice the pion mass, one expects that the pion would have to be treated as a long-range degree of freedom in a free-space EFT applicable to most nuclei. Chiral EFTs for nucleons incorporate the pion systematically as the (near) Goldstone boson of approximate and spontaneously broken chiral symmetry, expanding about the massless pion limit. The functional dependence on the QCD quark masses is captured in perturbation theory and the dependence on the strong coupling is contained in universal parameters to be determined from data or direct numerical calculations of QCD. Chiral EFT in nuclear physics originated with the seminal work of Weinberg and van Kolck and collaborators in the early 1990s (31–37), and the field has been active ever since (4–6).

Currently the most commonly applied chiral EFT Lagrangians have nonrelativistic nucleons and pions as degrees of freedom based on the "heavy-baryon" formalism, which eliminates antinucleons and organizes relativistic corrections (4). As usual, renormalization can be carried out because all interactions consistent with QCD symmetries are included, which allows regulator dependence to be absorbed. To organize the EFT in a systematic hierarchy we need a power counting, but the optimal scheme is not yet settled. Both practical and formal questions are being argued and different schemes are under investigation (38–42). In all cases, chiral symmetry dictates that pion interactions be accompanied by derivatives (because they are Goldstone bosons) or powers of the pion mass (Ward identity constraints from QCD), thus yielding ratios of characteristic momenta and m_π to the scale of excluded physics, such as heavier meson exchange, as expansion parameters. Relativistic corrections are organized in powers of momenta over the nucleon mass.

For applications to nuclear structure, an energy-independent nucleons-only potential is desirable (and required for many of the methods discussed below); it can be derived from the chiral Lagrangian by a unitary transformation method that decouples the nucleons from explicit pion fields, leaving static pion-exchange interactions and regulated contact terms (6). At present these potentials are organized by a power counting proposed by Weinberg, then iterated with either a Lippmann-Schwinger equation for two-body scattering or another nonperturbative method for bound-state properties with more nucleons. A momentum-space cutoff is used for technical reasons, which means that the advantages of dimensional regularization we saw for short-range interactions at finite density are not available.

For Weinberg power counting there is a formula analogous to Equation 11 that identifies the order in the EFT expansion at which a given term in the potential contributes. This formula yields a hierarchy of terms with increasing derivatives and pion exchanges and, perhaps most important for finite-density applications to be tractable, a hierarchy of many-body forces. At LO, there is one pion exchange and two no-derivative contact terms. The NLO adds the first two-pion exchange contributions, which are important for the mid-range nuclear attraction. At present, NN interactions go to up to N^3LO, which includes 24 constants for the contact terms (not including isospin violation) that are determined by fits to NN scattering. The best fits have a χ^2/dof comparable to the best phenomenological potentials (43, 44).

Three-nucleon forces (3NF) appear first at N^2LO and are shown on the left in **Figure 1**. There are parameters associated with long-range two-pion exchange (four constants fit to πN or NN scattering), mid-range one-pion exchange (one constant), and purely short-range (one constant) parts. The extension to N^3LO is in progress and involves many additional diagrams but no additional parameters. However, there are sizable uncertainties at present in determining the long-range 3NF parameters from πN or NN scattering, which translate into significant

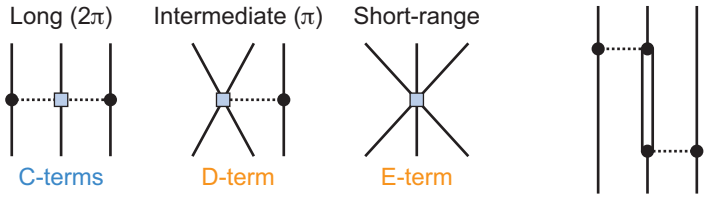

Figure 1

Leading three-body contributions in chiral effective field theory (EFT). *Left*: N^2LO terms in an EFT without Δs (dashed line represents the pion). *Right*: NLO contribution with explicit Δs (*double line*). Abbreviation: NLO, next-to-leading-order.

uncertainties at finite density. The four-nucleon (4N) interaction appears first at N^3LO in the form of long-range pion exchange and is parameter free (45). The quantitative suppression of many-nucleon forces predicted by chiral power counting is consistent with binding-energy calculations in light nuclei (6, 46), but much remains to be tested in larger systems.

Even after we specify a power counting and the order in the expansion, there is no unique EFT potential because one can choose different cutoffs. Calculations of observables should be independent of the cutoff at the level of the truncation error determined by the missing orders. By comparing calculations with varied cutoffs one can test whether the EFT is working and then put a bound on the theoretical error. The precision EFT potentials currently available for nuclear structure have cutoffs in a rather narrow range close to the expected breakdown scale of the EFT, about 450–600 MeV (cf. the ρ or ω meson mass), which is consistent with the prescription of Lepage (47, 48). In practice, lower cutoffs mean large truncation errors (i.e., the expansion parameter q/Λ_c gets too small), whereas larger cutoffs create implementation problems with increasingly singular (at short distances) potentials from multiple pion exchange. Within this cutoff range there is no penalty for iterating subleading potential terms, which violates some power countings, because the truncation and iteration errors are the same size (4).

Recent surveys of ongoing applications of chiral potentials to scattering and to properties of few-body nuclei can be found in References 4 and 6. Among the developments most relevant to finite density is work to add the Δ(1232)-isobar resonance explicitly to the chiral EFT Lagrangian; this research formed part of the original explorations by van Kolck et al. (35–37), but has only recently been reconsidered for energy-independent potentials (49, 50). The Δ is considered important because of its low excitation energy (the mass difference to the nucleon is about 300 MeV) and its strong coupling to the πN system. Including Δ would resum important contributions and improve the pattern of convergence. In this scheme, the leading 3NF term comes from pion exchange with an intermediate Δ (**Figure 1**, *right*) and appears at NLO. As this and other developments mature, in parallel there will be applications to finite nuclei. Indeed, because the energy-independent potentials take the same form as phenomenological nonlocal potentials, almost all conventional few- and many-body methods are immediately available.

3.2. Wave Function Methods

There are a wide variety of methods available to determine properties of few-body systems given an internucleon potential. Each in some way involves solving for the approximate wave function of the system. If we arbitrarily set the crossover from few-body to many-body nuclei at $A = 8$, the choice of methods dwindles to a few: Green's function Monte Carlo (GFMC), no-core shell model (NCSM), and coupled cluster (CC). The GFMC approach (51, 52) has had great success up to $A = 12$ (and extensions using auxiliary field methods promise to go much further), but is

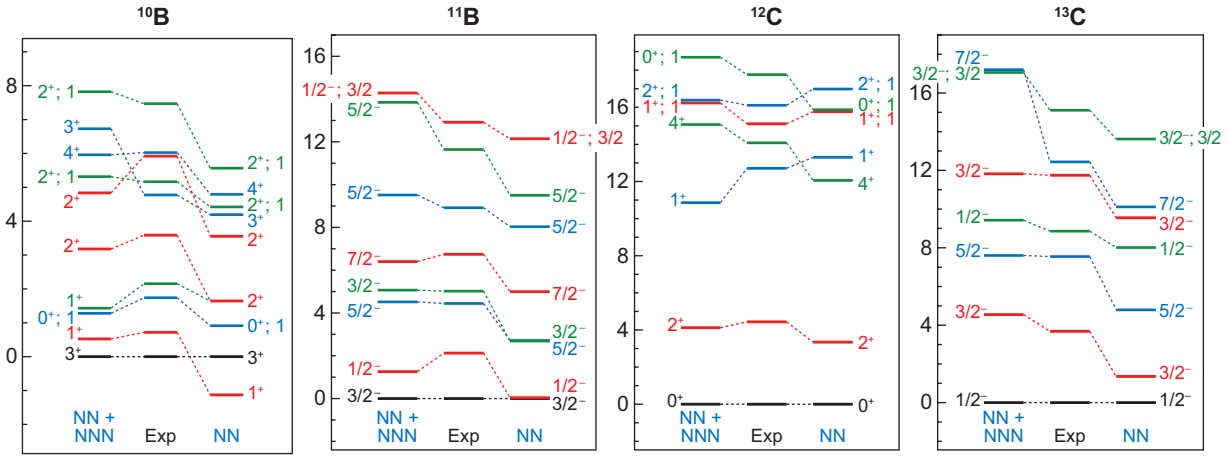

Figure 2

Excitation energies (in MeV) of selected levels in four *p*-shell nuclei (55) calculated using the N^{3}LO potential of Reference 43. Calculations with nucleon-nucleon- (NN-)only and with N^{3}LO NN plus N^{2}LO three-nucleon forces are compared to experiment. Abbreviation: NLO, next-to-leading-order.

limited at present to local potentials, i.e., diagonal in coordinate representation, which excludes current chiral EFT interactions. However, both the NCSM and CC methods are compatible with energy-independent chiral potentials including many-body forces (53, 54).

The NCSM diagonalizes the Hamiltonian in a harmonic oscillator basis with all nucleons active (hence no core). Lanczos methods allow the extraction of the lowest eigenvalues and eigenvectors from spaces up to dimension 10^9 (and growing, given the advances in computer hardware and software), but the matrix size grows rapidly with A and the maximum oscillator excitation energy $N_{\max}\hbar\Omega$. For a given A, the convergence of observables with $N_{\max}$ depends strongly on the nature of the potential. Chiral EFT Hamiltonians are softer than conventional nuclear potentials (i.e., smaller high-momentum contributions, which means less coupling to high oscillator states), but adequate convergence with 3NF still requires too large a basis beyond the lightest nuclei. Therefore Lee-Suzuki transformations of the potential, which are unitary order by order in a cluster expansion, are applied to decouple included and excluded oscillator states, greatly reducing the size of the model space needed. This procedure has many demonstrated successes (53, 55) although there are drawbacks, such as distortions of long-range physics, problems with extrapolations of energies, and the loss of the variational principle (56).

Recent state-of-the-art NCSM calculations of excitation energies for four *p*-shell nuclei are shown in **Figure 2** for a single N^{3}LO potential with and without the N^{2}LO 3NF (55). (The mismatch in orders means that this calculation is not yet completely consistent from the EFT perspective.) It is evident that the fine structure of the nuclear spectra is uniformly improved with the three-body contribution. Of particular note is the ground state of ^{10}B and the splittings of spin-orbit partners throughout. The sensitivity of three-body parameters to particular observables (e.g., ^{6}Li quadrupole moment, the lowest 1^+ states in ^{10}B) suggests that fits of 3NF parameters will improve with input from more than $A = 3, 4$ systems (55).

How can we tell if an EFT-based interaction used by a wave function method is working as expected? One way is to do comparative calculations at different orders in the EFT with a range of cutoffs. Because cutoff variation is absorbed by the contact interactions, which scale as powers of

the inverse cutoff, the relative variation of the potential energies over this range should decrease systematically according to the power of omitted contact interactions (and assuming a typical momentum scale ≈130 MeV). Binding-energy variations will be larger because of cancellations in nuclear systems, which amplify the role of higher orders (including many-body forces). Nogga has shown that such estimates are consistent with calculations in ^{3}H (57). For ^{4}He, he concludes that the EFT estimate of 2% for the ratio of 3NF to NN potential energies is consistent with observed ratios of roughly 5% (57), and preliminary calculations of the 4NF contribution were found to be as small as expected (46). All of these tests will need to be repeated for larger nuclei as reliable calculations become possible.

RG methods applied in free space to chiral EFT interactions are a promising means of calculating larger nuclei. These methods prescribe how each matrix element of the potential (and other operators) in a discretized momentum basis must evolve under changes in the resolution scale so that observables remain unchanged. (Because the potential is not an observable, we are always free to make unitary transformations.) The resolution scale is changed by lowering a cutoff in relative momentum ($V_{\mathrm{low}\,k}$) (58), by using a flow equation for the Hamiltonian (similarity RG) (59) or by using tailored unitary transformations (UCOM) (60). The result is a decoupling of high- and low-momentum dependence without modification of long-distance interactions, leading to low-momentum potentials that are more perturbative, such that convergence in harmonic oscillator bases is dramatically accelerated (61). Such potentials can be applied without Lee-Suzuki transformations in the NCSM and can maintain the variational principle. Because the transformations are unitary, the EFT truncation error is unchanged, in contrast to the RG evolution of a chiral EFT at fixed order to low cutoff. However, the evolution of the NN potential is inevitably accompanied by the evolution of the three- and higher-body potentials. The latter has not yet been implemented but is instead approximated by fitting the N^{2}LO chiral interaction at each cutoff (62), which introduces a theoretical error.

These low-momentum potentials show great promise for the CC method, which has been highly developed in ab initio quantum chemistry but has only recently been revived for nuclear applications, including the development of CC theory for three-body Hamiltonians (54, 63). CC calculations are based on a potent exponential ansatz for the ground-state wave function $|\psi\rangle = e^{\hat{T}}|\phi\rangle$, where $|\phi\rangle$ is a simple reference state (typically a harmonic oscillator Slater determinant). The operator $\hat{T}$ is specified by amplitudes for a truncated sum of operators creating one-particle–one-hole, two-particle–two-hole, etc. excitations. The amplitudes are found from nonlinear equations whose solution scales vary gently with the size of the nucleus and model space.

As with the NCSM, convergence is accelerated with low-momentum potentials; particularly promising is the calculation of 3NF contributions, which are the most expensive component. The 3NF potential is rewritten in terms of normal-ordered creation and destruction operators with respect to $|\phi\rangle$ (instead of the vacuum), which recasts the 3NF into an expectation value in $|\phi\rangle$, one- and two-body pieces, and the remaining 3NF part. In the hierarchy of contributions to a CC calculation, only the last piece is expensive to calculate, but recent CC calculations of ^{4}He found it to be negligible (54). If this result persists for larger nuclei, calculations of $A = 100$ or beyond will be feasible in the near future! The present limit for NCSM is much lower, around $A = 16$, but could be extended using importance-sampling methods that select the most important basis states (64), if such methods can be implemented in a size-extensive way.

The NCSM and CC wave function methods apply EFT (and RG) only to create the input potential and not to solve the many-body problem. There is also the possibility of a more EFT-like treatment, such as the pioneering work to apply EFT to the shell model by Stetcu et al. (65). (See Reference 66 for a completely different application of EFT methods to the shell model.) These authors formulate an EFT in the harmonic oscillator basis, where the restricted model

space generates all interactions consistent with the underlying symmetries. The parameters are directly determined in the model space rather than fitting in free space and transforming the interaction. The oscillator frequency sets an infrared cutoff $\lambda \sim \sqrt{M_N \hbar\Omega}$ whereas the UV cutoff is $\Lambda \sim \sqrt{M_N(N_{\max}+3/2)\hbar\Omega}$. Within each model space, a set of observables is used to fix the EFT parameters, then other observables are calculated. The EFT works if cutoff dependence decreases with decreasing λ and increasing Λ; in that case one makes an extrapolation to the continuum limit $\hbar\Omega \to 0$ with $N_{\max} \to 0$ with Λ fixed. At the end, one takes $\Lambda \to \infty$. The first application with a pionless theory up to $A = 6$ is encouraging and motivates generalizations to the pionful theory and to other many-body methods (65).

3.3. Effective Field Theory on the Lattice

We have seen that chiral EFT potentials have been used successfully in connection with standard numerical many-body approaches such as CC or the NCSM. A disadvantage of these methods is that they rely on the existence of a potential, which is not an observable, and as a consequence scheme and renormalization scale invariance are not manifest. A numerical few- and many-body method that is based directly on the effective Lagrangian is the Euclidean lattice path integral Monte Carlo method. Euclidean lattice calculations are standard in the context of QCD but, except for some isolated attempts (67, 68), have been applied in nuclear physics only recently (69–71).

In the following paragraphs we introduce the Euclidean lattice method in the case of a simple s-wave contact interaction $\mathcal{L} = -C_0(\psi^\dagger\psi)^2/2$. More sophisticated interactions involving higher partial-wave terms and explicit pions are discussed in Reference 72. The usual strategy for dealing with the four-fermion interaction is to use a Hubbard-Stratonovich transformation. The partition function can be written (69) as

$$Z = \int Ds\ Dc\ Dc^*\ \exp[-S], \tag{36.}$$

where s is the Hubbard-Stratonovich field and c is a Grassmann field. S is a discretized Euclidean action

$$\begin{aligned} S = \sum_{\mathbf{n},i} \Big[e^{-\hat{\mu}\alpha_t} c_i^*(\mathbf{n}) c_i(\mathbf{n}+\hat{\mathbf{0}}) - e^{\sqrt{-C_0\alpha_t}s(\mathbf{n}) + \frac{C_0\alpha_t}{2}} (1-6h) c_i^*(\mathbf{n}) c_i(\mathbf{n}) \Big] \\ - h \sum_{\mathbf{n},\mathbf{l}_s,i} [c_i^*(\mathbf{n}) c_i(\mathbf{n}+\hat{\mathbf{l}}_s) + c_i^*(\mathbf{n}) c_i(\mathbf{n}-\hat{\mathbf{l}}_s)] + \frac{1}{2}\sum_{\mathbf{n}} s^2(\mathbf{n}). \end{aligned} \tag{37.}$$

Here i labels spin and $\mathbf{n}$ labels lattice sites. Spatial and temporal unit vectors are denoted by $\hat{\mathbf{l}}_s$ and $\hat{\mathbf{0}}$, respectively. The temporal and spatial lattice spacings are b_τ and b, and the dimensionless chemical potential is given by $\hat{\mu} = \mu b_\tau$. We define α_t as the ratio of the temporal and spatial lattice spacings and $h = \alpha_t/(2\hat{m})$. The action (37) is quadratic in the fermion fields, and can be simulated using a variety of methods such as determinant or hybrid Monte Carlo. Note that for $C_0 < 0$ the action is real and importance sampling is possible.

The four-fermion coupling is fixed by computing the sum of all particle-particle bubbles as in Section 2.3, but with the elementary loop function regularized on the lattice. Schematically,

$$\frac{m}{4\pi a_0} = \frac{1}{C_0} + \frac{1}{2}\sum_{\mathbf{p}} \frac{1}{E_{\mathbf{p}}}, \tag{38.}$$

where the sum runs over discrete momenta on the lattice and $E_{\mathbf{p}}$ is the lattice dispersion relation. A detailed discussion of the lattice regularized scattering amplitude can be found in References 69, 74, and 75. For a given scattering length a_0 the four-fermion coupling is a function of the lattice

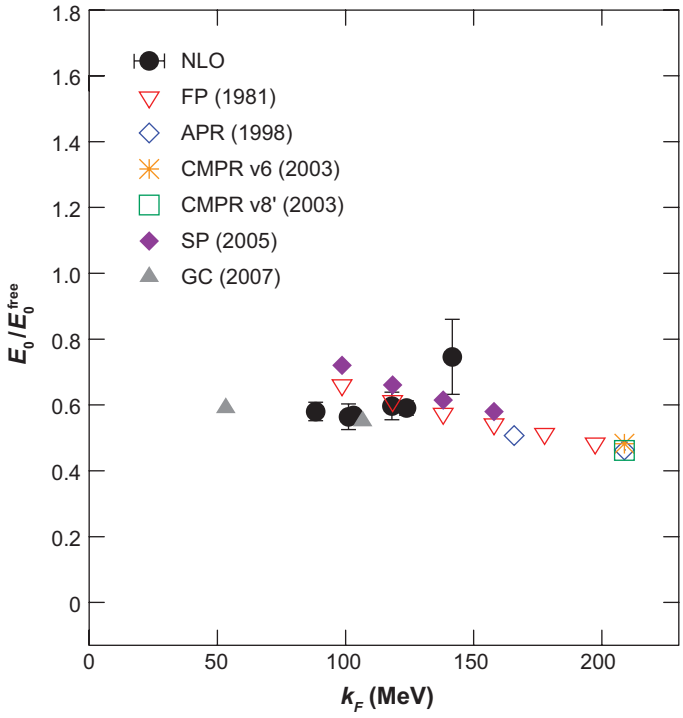

Figure 3

Lattice results for the energy per particle of a dilute Fermi gas from Borasoy et al. (72, 73). We show the energy per particle in units of the same ratio for the free system as a function of the Fermi momentum. The solid dots represent the lattice results. For comparison, we also show results from wave function–based many-body calculations (72). Abbreviation: NLO, next-to-leading-order.

spacing. The continuum limit corresponds to taking the temporal and spatial lattice spacings b_τ, b to zero,

$$b_\tau \mu \to 0, \quad b n^{1/3} \to 0, \tag{39.}$$

keeping $a_0 n^{1/3}$ fixed. Here μ is the chemical potential and n is the density. Numerical results for the energy per particle of dilute neutron matter are shown in **Figure 3**. We observe that the results agree quite well with traditional many-body calculations. We also note that even when higher-order corrections are taken into account, the equation of state exhibits approximate universal behavior, with an effective $\xi \simeq (0.5-0.6)$. For applications of the lattice method to finite nuclei, see Reference 76.

3.4. Perturbative Effective Field Theory for Nuclear Matter

The nuclear calculations discussed so far have all been nonperturbative. However, RG methods have been used to show that the perturbativeness of internucleon interactions depends strongly on the momentum cutoff and the density (58, 77). Lowering the resolution via an RG evolution leaves observables and EFT truncation errors unchanged by construction (up to approximation errors and omitted many-body contributions) but shifts contributions between the potential and the sums over intermediate states in loop integrals. These shifts can weaken or even eliminate sources of nonperturbative behavior such as strong short-range repulsion (e.g., from singular

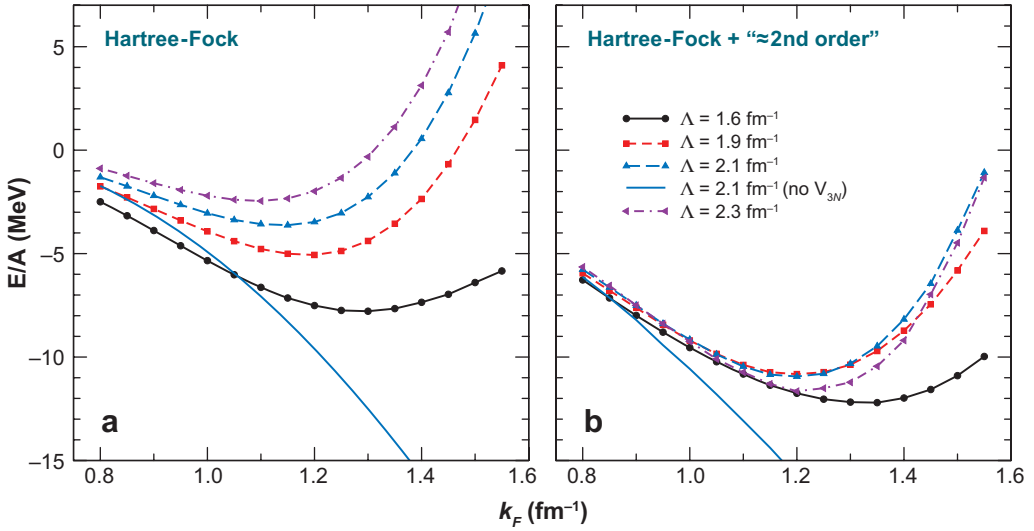

Figure 4

Nuclear matter energy per particle using renormalization-group evolved low-momentum potentials with a range of cutoffs with three-nucleon forces fit to few-body binding energies (78).

chiral two-pion exchange) or the tensor force. At sufficient density, effective range corrections and beyond suppress the effects of large *s*-wave scattering lengths (78).

Consequently, although nuclear matter is generally considered to be nonperturbative, it is also resolution dependent. **Figure 4** shows the energy per particle in nuclear matter for several values of the RG cutoff Λ calculated in leading-order (Hartree-Fock) and second-order many-body perturbation theory (78). (Note: The initial potential used in these figures is not a chiral EFT NN potential. However, all NN potentials fit to scattering phase shifts flow to very similar low-momentum potentials by this range of cutoffs, so similar results are expected.) The three-body potential is of the N^{2}LO form, fit at each cutoff to the binding energies of the triton and ^{4}He. As the RG only changes short-distance physics, the procedure for determining the 3NF is argued to be a good approximation to the consistently evolved 3NF (62).

There are several encouraging features of perturbative many-body calculations with RG evolved potentials. First, Hartree-Fock is a reasonable starting point for the description of nuclear matter; this is patently false for conventional phenomenological potentials, which do not even bind. Second, the dependence on the cutoff is greatly reduced going to second order. Further calculations show that the third-order ladder diagrams make a very small contribution (78). Third, with a fit to few-body properties, the minimum is reasonably close to the empirical saturation point of (roughly) 16 MeV per particle with $k_F \approx 1.35$ fm^{-1} (indeed, the discrepancy is the order of uncertainties in the three-body force). These results motivate a program to study nuclear matter with chiral EFT internucleon forces evolved to lower resolution (which should also include studying unevolved chiral EFT potentials fit with a lower cutoff).

The increased perturbativeness in nuclear matter with increased density and lower cutoff can be understood physically from reduced phase space due to Pauli blocking and the cutoff, combined with the favorable momentum dependence of the low-momentum interaction (77, 78). Pauli blocking means that particles with momenta below k_F must forward scatter (Hartree-Fock) or be excited out of the Fermi sea. The latter amplitude is limited by the weakened coupling of occupied and unoccupied states, which in turn limits the volume of available momentum states (this is the

phase space restriction). A consequence is that the saturation mechanism is now dominated by the three-body force contribution (cf. the NN-only curves in the figure), rather than by the density dependence of two-body tensor contributions. For cutoffs in the range shown, the three-body contribution still remains natural-sized according to chiral EFT power counting (78), but it is clearly quantitatively important. The implication is that the 4NF contribution will also be important at the level of about 1 MeV per particle at saturation, but this conjecture has yet to be tested.

These results suggest that an alternative EFT power counting may be appropriate at nuclear matter densities. Kaiser and collaborators have proposed a perturbative chiral EFT approach to nuclear matter and then to finite nuclei through an energy functional (79–81; see also 82, 84). They consider Lagrangians both for nucleons and pions and for nucleons, pions, and Δs, and fit parameters to nuclear saturation properties. They construct a loop expansion for the nuclear matter energy per particle, which leads to an energy expansion of the form

$$E(k_{\rm F}) = \sum_{n=2}^{\infty} k_{\rm F}^n \, f_n(k_{\rm F}/m_\pi,\ \Delta/m_\pi), \quad [\Delta = M_\Delta - M_N \approx 300\,{\rm MeV}] \tag{40.}$$

where each f_n is determined from a finite number of in-medium Feynman diagrams. All powers of $k_{\rm F}/m_\pi$ and Δ/m_π are kept in the f_ns because these ratios are not small quantities (83). A semi-quantitative description of nuclear matter is found even with just the lowest two terms without Δs, and adding Δs brings uniform improvement (e.g., in the neutron matter equation of state). There remain open questions about power counting and convergence, and there are many promising avenues to pursue.

3.5. Density Functional Theory as an Effective Field Theory

DFT (85–87) is widely used in condensed-matter and quantum chemistry to treat large many-body systems. It is based on the response of the ground-state energy to external perturbations of the density, with fermion densities as the fundamental variables. This means that the computational cost for DFT is far less than for wave function methods, and the calculations can be applied to heavy nuclei. DFT is naturally formulated in an effective action framework (88) and is carried out using an inversion method implemented with EFT power counting (89–91).

The simple prototype EFT for a dilute system (see Section 2) can be revisited in DFT by placing the fermions in a trap potential $v_{\rm ext}(\mathbf{x})$ (e.g., a harmonic oscillator) and adding sources coupled to external densities (92). Consider a single external source $J(\mathbf{x})$ coupled to the density operator $\hat{\rho}(x) \equiv \psi^\dagger(x)\psi(x)$ in the partition function (neglecting normalization and factors of the temperature and volume and suppressing $v_{\rm ext}$),

$$\mathcal{Z}[J] = e^{-W[J]} \sim {\rm Tr}\, e^{-\beta(\hat{H}+J\hat{\rho})} \sim \int \mathcal{D}[\psi^\dagger]\mathcal{D}[\psi]\, e^{-\int[\mathcal{L}+J\psi^\dagger\psi]}, \tag{41.}$$

with the Lagrangian from Section 2.1. The static density $\rho(\mathbf{x})$ in the presence of $J(\mathbf{x})$ is

$$\rho(\mathbf{x}) \equiv \langle\hat{\rho}(\mathbf{x})\rangle_J = \frac{\delta W[J]}{\delta J(\mathbf{x})}, \tag{42.}$$

which we invert to find $J[\rho]$ and then Legendre transform from J to ρ:

$$\Gamma[\rho] = -W[J] + \int d^3x J(\mathbf{x})\rho(\mathbf{x}) \quad \text{with} \quad J(\mathbf{x}) = \frac{\delta\Gamma[\rho]}{\delta\rho(\mathbf{x})} \to \left.\frac{\delta\Gamma[\rho]}{\delta\rho(\mathbf{x})}\right|_{\rho_{\rm gs}(\mathbf{x})} = 0. \tag{43.}$$

For static $\rho(\mathbf{x})$, $\Gamma[\rho]$ is proportional to the Hohenberg-Kohn energy functional, which by Equation 43 is extremized at the ground state density $\rho_{\rm gs}(\mathbf{x})$.

With $W[J]$ constructed as a diagrammatic expansion, EFT power counting provides us with a means of inverting from $W[J]$ to $\Gamma[\rho]$ (89, 90). It proceeds by substituting the decomposition $J(\mathbf{x}) = J_0(\mathbf{x}) + J_1(\mathbf{x}) + J_2(\mathbf{x}) + \ldots$ (where 1 stands for LO, 2 stands for NLO, and so on) and corresponding expansions for W and Γ into Equation 43 and matching order by order with ρ treated as order unity. Here J_0 is chosen so that there are no corrections to the zeroth order density at each order in the expansion; the interpretation is that J_0 is the external potential that yields for a noninteracting system the exact density of the interacting system. Zeroth order is the noninteracting system with potential $J_0(x)$,

$$\Gamma_0[\rho] = -W_0[J_0] + \int d^3x\, J_0(\mathbf{x})\rho(\mathbf{x}) \Rightarrow \rho(\mathbf{x}) = \frac{\delta W_0[J_0]}{\delta J_0(\mathbf{x})}, \qquad 44.$$

which is the so-called Kohn-Sham system with the exact density! To evaluate $W_0[J_0]$, we introduce orbitals $\{\psi_\alpha\}$ satisfying (with v_{ext} made explicit)

$$\left[-\frac{\nabla^2}{2M} + v_{\text{ext}}(\mathbf{x}) - J_0(\mathbf{x})\right]\psi_\alpha(\mathbf{x}) = \varepsilon_\alpha\psi_\alpha(\mathbf{x}), \qquad 45.$$

which diagonalizes W_0, so that it yields a sum of ε_αs for the occupied states. We calculate the W_is and Γ_is up to a given order as functionals of J_0 and then determine J_0 for the ground state via a self-consistency loop:

$$J_0 \to W_1 \to \Gamma_1 \to J_1 \to W_2 \to \Gamma_2 \to \cdots \Rightarrow J_0(\mathbf{x})|_{\rho=\rho_{\text{gs}}} = \left.\frac{\delta\Gamma_{\text{interacting}}[\rho]}{\delta\rho(\mathbf{x})}\right|_{\rho=\rho_{\text{gs}}}. \qquad 46.$$

Adding sources coupled to other currents improves the functional variationally and allows pairing to be treated within the same framework (93, 94).

Figure 5 shows how EFT power-counting estimates predict the hierarchy of contributions to a DFT energy functional. Shown at left are the results for the energy per particle of $A = 140$ fermions in a trap with short-range repulsive interactions. The a priori estimates from terms at three different orders in the EFT expansion (the counterparts to the terms in Equation 2 plus gradient corrections) are shown with error bars that reflect a natural range for the unknown coefficients (in this case from 1/2 to 2). These are compared to actual values, with good agreement (93). A similar exercise using a chiral EFT–inspired power counting has been applied to phenomenological nonrelativistic (Skyrme) and covariant density functionals. Results for terms organized by powers of the density in each term are shown on the right in **Figure 5** and show that the predicted hierarchy is realized (91, 95).

The apparent success of many-body perturbation theory for nuclear matter using low-momentum potentials RG-evolved from chiral EFT input enables the construction of a nuclear DFT functional in the effective action formalism that is compatible with nonrelativistic Skyrme energy functional technology (96, 97). A large-scale five-year project to develop a universal nuclear energy density functional (UNEDF) that will cover the entire table of nuclides (98) is under way. The goal is to generate systematically improved energy functionals based on chiral EFT/RG input potentials, including theoretical error estimates so that extrapolation to the driplines is under control.

The density matrix expansion (DME) of Negele & Vautherin (99, 100) has been extended to three-body force contributions and applied in momentum space to provide the first-generation functional (91, 101). This construction is facilitated by analytic expressions for the long-range pion contributions derived by Kaiser et al. (80, 81). The functional has the form of a generalized Skyrme functional with density-dependent coefficients, including all allowed terms up to two derivatives, which means it can be directly incorporated into existing computer codes. Cutoff dependence can be used as a diagnostic tool for assessing missing elements of the interaction, the many-body

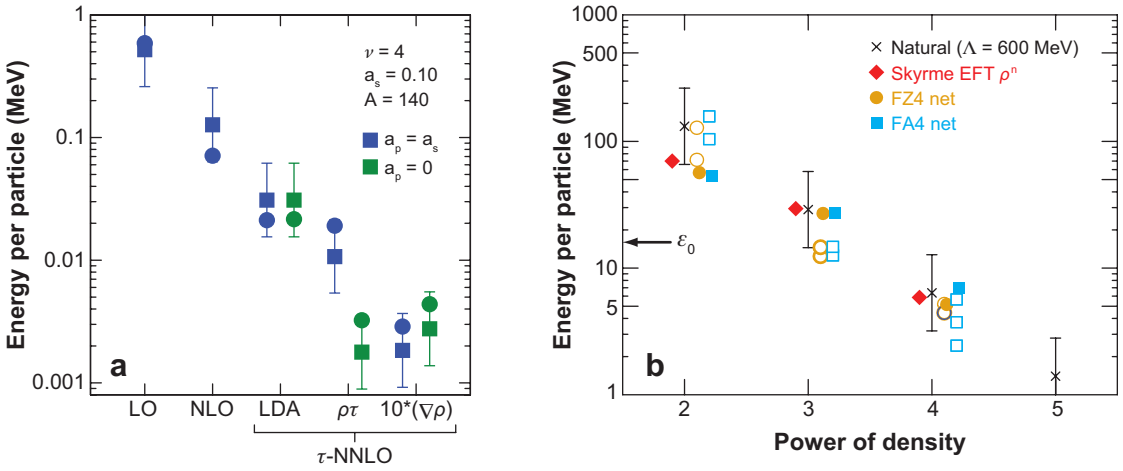

Figure 5

Estimates for energy functionals for a dilute fermion in a harmonic trap (*a*) and three phenomenological energy functionals for nuclei (*b*).

approximations, and the performance of the energy functional. It is possible to benchmark against NCSM and CC calculations for light- and medium-mass nuclei by calculating the energy with an additional external field, i.e., putting the nuclei in theoretically adjustable traps.

4. SUMMARY AND OUTLOOK

EFT is a well-established technique with demonstrated success in all branches of physics. Applications of EFT to finite-density systems have many precursors going back decades, but implementations are relatively recent. Many-body systems with short-range interactions are an ideal testing ground for many-body EFT because of the universal nature of the systems and the connection to experiment through cold atom physics.

Far less developed is the application of EFT methods to nuclear many-body systems. The immediate impact of EFT on nuclear many-body calculations is through the systematic organization of effective Hamiltonians for low-energy QCD using chiral EFT. Of particular importance is the role of many-body forces. We emphasize that although these Hamiltonians have been successful in describing scattering and properties of light nuclei, they are largely untested at the densities that are relevant for most nuclei and nuclear matter. Fortunately, computational tools such as the NCSM, CC, and lattice methods, RG techniques, and DFT will funnel advances in chiral EFT to new predictions, so that true tests are forthcoming. More direct applications of EFT methods to many-body calculations are in their infancy, but there are clear incentives to pursue them.

This has necessarily been a shallow survey, but the breadth of activity should be clear. Key developments are expected in the next few years. These include improvements to the chiral EFT potentials such as full N^3LO three-body interactions and the corresponding N^3LO Hamiltonian with Δ degrees of freedom and the subsequent testing of power counting in light- to medium-mass systems. In addition, the consistent evolution of many-body forces with RG methods will open the door to the full range of nuclei and nuclear matter.

Beyond the calculational tools, EFT provides a new perspective for nuclear many-body calculations. Whereas traditionally one sought a universal Hamiltonian for all problem and energy length scales, EFT exploits the infinite number of low-energy potentials: Rather than finding the

"best" potential, we use a convenient or efficient one or work directly from a Lagrangian. For a long time it was hoped that two-body data would be sufficient for nuclear systems; many-body forces were treated as a last resort, to be considered as an add-on. In EFT it is inevitable that many-body forces and data are needed and that they are directly tied to the two-body interaction. Whereas researchers used to avoid divergences and hide them in form factors, with EFT they now confront and exploit them (e.g., using cutoff dependence as a tool). Finally, instead of choosing diagrams to sum by "art," power counting determines what to sum and establishes theoretical truncation errors.

Many relevant and interesting topics were not treated here because of space limitations. Two major (related) areas largely unaddressed are (*a*) the response to external probes and (*b*) nuclear reactions. Another area is EFT at high temperature for many-body systems with large scattering length, which has been formulated using the virial expansion (102, 103) (see References 104 and 105 for recent applications of the virial expansion to hot dilute nuclear matter). The EFT formulation of the finite temperature nuclear many-body system with long-range pion interaction is a frontier. Other nuclear systems wherein EFT can play a particular role are hypernuclei (57) and halo nuclei (106). Work to apply EFT methods to covariant hadronic field theories strives to understand the successes of relativistic mean-field phenomenology (107). Finally, there is the challenge of making the connection to lattice QCD (108) (as opposed to EFT on the lattice).

DISCLOSURE STATEMENT

The authors are not aware of any biases that might be perceived as affecting the objectivity of this review.

ACKNOWLEDGMENTS

This work was supported in part by the National Science Foundation under grant nos. PHY-0354916 and PHY-0653312, the Department of Energy under grant no. DE-FG02-03ER4126, and the UNEDF SciDAC Collaboration under DOE grant DE-FC02-07ER41457.

LITERATURE CITED

1. Natl. Res. Counc. *Nuclear Physics: The Core of Matter, the Fuel of Stars*. Washington, DC: Natl. Acad. (1999)
2. Burgess CP. *Annu. Rev. Nucl. Part. Sci.* 57:329 (2007)
3. Bernard V, Meißner U-G. *Annu. Rev. Nucl. Part. Sci.* 57:33 (2007)
4. Bedaque PF, van Kolck U. *Annu. Rev. Nucl. Part. Sci.* 52:339 (2002)
5. Beane SR, et al. nucl-th/0008064 (2000)
6. Epelbaum E. *Prog. Part. Nucl. Phys.* 57:654 (2006)
7. Fetter AL, Walecka JD. *Quantum Many-Particle Systems*. New York: McGraw-Hill (1971)
8. Hammer HW, Furnstahl RJ. *Nucl. Phys. A* 678:277 (2000)
9. Negele JW, Orland H. *Quantum Many-Particle Systems*. Redwood City, CA: Addison-Wesley (1988)
10. Braaten E, Nieto A. *Phys. Rev. B* 56:14745 (1997)
11. Pines D. *The Theory of Quantum Liquids*. Menlo Park, CA: Addison-Wesley (1966)
12. Baym G, Pethick C. *Landau Fermi Liquid Theory*. New York: Wiley (1991)
13. Abrikosov AA, Gorkov LP, Dzyaloshinski IE. *Methods of Quantum Field Theory in Statistical Physics*. Englewood Cliffs, NJ: Prentice Hall (1963)
14. Shankar R. *Rev. Mod. Phys.* 66:129 (1994)
15. Polchinski J. hep-th/9210046 (1992)
16. Papenbrock T, Bertsch GF. *Phys. Rev. C* 59:2052 (1999)

17. Marini M, Pistolesi F, Strinati GC. *Eur. Phys. J. B* 1:151 (1998)
18. Wambach J, Ainsworth TL, Pines D. *Nucl. Phys. A* 555:128 (1993)
19. Gorkov LP, Melik-Barkhudarov TK. *Sov. Phys. JETP* 13:1018 (1961)
20. Schwenk A, Friman B, Brown GE. *Nucl. Phys. A* 713:191 (2003)
21. Kaplan DB, Savage MJ, Wise MB. *Nucl. Phys. B* 534:329 (1998)
22. Regal C. *Experimental realization of BCS-BEC crossover physics with a Fermi gas of atoms*. PhD thesis. Univ. Colo., Boulder (2005)
23. Furnstahl RJ, Hammer HW. *Ann. Phys.* 302:206 (2002)
24. Nikolic P, Sachdev S. *Phys. Rev. A* 75:033608 (2007)
25. Steele JV. nucl-th/0010066 (2000)
26. Schäfer T, Kao CW, Cotanch SR. *Nucl. Phys. A* 762:82 (2005)
27. Rupak G. nucl-th/0605074 (2006)
28. Nussinov Z, Nussinov S. *Phys. Rev. A* 74:053622 (2006)
29. Nishida Y, Son DT. *Phys. Rev. Lett.* 97:050403 (2006)
30. Arnold P, Drut JE, Son DT. *Phys. Rev. A* 75:043605 (2007)
31. Weinberg S. *Phys. Lett. B* 251:288 (1990)
32. Weinberg S. *Nucl. Phys. B* 363:3 (1991)
33. Ordonez C, van Kolck U. *Phys. Lett. B* 291:459 (1992)
34. Weinberg S. *Phys. Lett. B* 295:114 (1992)
35. Ordonez C, Ray L, van Kolck U. *Phys. Rev. Lett.* 72:1982 (1994)
36. van Kolck U. *Phys. Rev. C* 49:2932 (1994)
37. Ordonez C, Ray L, van Kolck U. *Phys. Rev. C* 53:2086 (1996)
38. Beane SR, Bedaque PF, Savage MJ, van Kolck U. *Nucl. Phys. A* 700:377 (2002)
39. Nogga A, Timmermans RGE, van Kolck U. *Phys. Rev. C* 72:054006 (2005)
40. Birse MC. *Phys. Rev. C* 74:014003 (2006)
41. Epelbaum E, Meißner U-G. nucl-th/0609037 (2006)
42. Pavon Valderrama M, Ruiz Arriola E. *Phys. Lett. B* 580:149 (2004)
43. Entem DR, Machleidt R. *Phys. Rev. C* 68:041001 (2003)
44. Epelbaum E, Glockle W, Meißner U-G. *Nucl. Phys. A* 747:362 (2005)
45. Epelbaum E. *Eur. Phys. J. A* 34:197 (2007)
46. Rozpedzik D, et al. *Acta Phys. Polon. B* 37:2889 (2006)
47. Lepage GP. In *Proc. TASI 1989*: *From Actions to Answers*, ed. T DeGrand, D. Toussaint, 23 pp. Singapore: World Sci. (1990)
48. Lepage GP. nucl-th/9706029 (1997)
49. Krebs H, Epelbaum E, Meißner U-G. *Eur. Phys. J. A* 32:127 (2007)
50. Epelbaum E, Krebs H, Meißner U-G. arXiv:0712.1969 (2007)
51. Pieper SC. *Nucl. Phys. A* 751:516 (2005)
52. Pieper SC. arXiv:0711.1500 (2007)
53. Nogga A, Navratil P, Barrett BR, Vary JP. *Phys. Rev. C* 73:064002 (2006)
54. Hagen G, et al. *Phys. Rev. C* 76:044305 (2007)
55. Navratil P, et al. *Phys. Rev. Lett.* 99:042501 (2007)
56. Stetcu I, Barrett BR, Navratil P, Vary JP. *Phys. Rev. C* 73:037307 (2006)
57. Nogga A. nucl-th/0611081 (2006)
58. Bogner SK, Kuo TTS, Schwenk A. *Phys. Rep.* 386:1 (2003)
59. Bogner SK, Furnstahl RJ, Perry RJ. *Phys. Rev. C* 75:061001 (2007)
60. Roth R, et al. *Phys. Rev. C* 72:034002 (2005)
61. Bogner SK, et al. *Nucl. Phys. A* 801:21 (2008)
62. Nogga A, Bogner SK, Schwenk A. *Phys. Rev. C* 70:061002 (2004)
63. Hagen G, et al. *Phys. Rev. C* 76:034302 (2007)
64. Roth R, Navratil P. *Phys. Rev. Lett.* 99:092501 (2007)
65. Stetcu I, Barrett BR, van Kolck U. *Phys. Lett. B* 653:358 (2007)
66. Haxton WC. arXiv:0710.0289 (2007)
67. Brockmann R, Frank J. *Phys. Rev. Lett.* 68:1830 (1992)

68. Muller HM, Koonin SE, Seki R, van Kolck U. *Phys. Rev. C* 61:044320 (2000)
69. Lee D, Schäfer T. *Phys. Rev. C* 72:024006 (2005)
70. Lee D, Schäfer T. *Phys. Rev. C* 73:015202 (2006)
71. Seki R, van Kolck U. *Phys. Rev. C* 73:044006 (2006)
72. Borasoy B, et al. arXiv:0712.2990 (2007)
73. Borasoy B, Epelbaum E, Krebs H, Lee D, Meissner U-G. nucl-th/0712.2993 (2007)
74. Chen JW, Kaplan DB. *Phys. Rev. Lett.* 92:257002 (2004)
75. Beane SR, Bedaque PF, Parreno A, Savage MJ. *Phys. Lett. B* 585:106 (2004)
76. Borasoy B, et al. *Eur. Phys. J. A* 31:105 (2007)
77. Bogner SK, Furnstahl RJ, Ramanan S, Schwenk A. *Nucl. Phys. A* 773:203 (2006)
78. Bogner SK, Schwenk A, Furnstahl RJ, Nogga A. *Nucl. Phys. A* 763:59 (2005)
79. Kaiser N, Fritsch S, Weise W. *Nucl. Phys. A* 697:255 (2002)
80. Kaiser N, Fritsch S, Weise W. *Nucl. Phys. A* 724:47 (2003)
81. Fritsch S, Kaiser N, Weise W. *Nucl. Phys. A* 750:259 (2005)
82. Lutz M, Friman B, Appel C. *Phys. Lett. B* 474:7 (2000)
83. Kaiser N, Muhlbauer M, Weise W. *Eur. Phys. J. A* 31:53 (2007)
84. Saviankou P, Krewald S, Epelbaum E, Meissner U-G. nucl-th/0802.3782 (2008)
85. Dreizler RM, Gross E. *Density Functional Theory*. Berlin: Springer-Verlag (1990)
86. Argaman N, Makov G. *Am. J. Phys.* 68:69 (2000)
87. Fiolhais C, Nogueira F, Marques M, eds. *A Primer in Density Functional Theory*. Berlin: Springer-Verlag (2003)
88. Polonyi J, Sailer K. *Phys. Rev. B* 66:155113 (2002)
89. Fukuda R, Kotani T, Suzuki Y, Yokojima S. *Prog. Theor. Phys.* 92:833 (1994)
90. Valiev M, Fernando GW. *Phys. Lett. A* 227:265 (1997)
91. Furnstahl RJ. nucl-th/0702040 (2007)
92. Puglia SJ, Bhattacharyya A, Furnstahl RJ. *Nucl. Phys. A* 723:145 (2003)
93. Bhattacharyya A, Furnstahl RJ. *Nucl. Phys. A* 747:268 (2005)
94. Furnstahl RJ, Hammer HW, Puglia SJ. *Ann. Phys.* 322:2703 (2007)
95. Furnstahl RJ. *J. Phys. G* 31:S1357 (2005)
96. Dobaczewski J, Nazarewicz W, Reinhard PG. *Nucl. Phys. A* 693:361 (2001)
97. Bender M, Heenen PH, Reinhard PG. *Rev. Mod. Phys.* 75:121 (2003)
98. Bertsch GF, Dean DJ, Nazarewicz W. *SciDAC Rev.* 6:42 (2007)
99. Negele JW, Vautherin D. *Phys. Rev. C* 5:1472 (1972)
100. Negele JW, Vautherin D. *Phys. Rev. C* 11:1031 (1975)
101. Bogner SK, Furnstahl RJ, Platter L. Manuscript in preparation (2008)
102. Bedaque PF, Rupak G. *Phys. Rev. B* 67:174513 (2003)
103. Rupak G. *Phys. Rev. Lett.* 98:090403 (2007)
104. Horowitz CJ, Schwenk A. *Nucl. Phys. A* 776:55 (2006)
105. Horowitz CJ, Schwenk A. *Phys. Lett. B* 638:153 (2006)
106. Bertulani CA, Hammer HW, Van Kolck U. *Nucl. Phys. A* 712:37 (2002)
107. Furnstahl RJ. *Lect. Notes Phys.* 641:1 (2004)
108. Savage MJ. nucl-th/0611038 (2006)

Annual Review of Nuclear and Particle Science

Volume 58, 2008

Contents

Indexes

Errata

An online log of corrections to *Annual Review of Nuclear and Particle Science* articles may be found at http://nucl.annualreviews.org/errata.shtml